Published in final edited form as:

*Dev Cell*. 2015 July 27; 34(2): 192–205. doi:10.1016/j.devcel.2015.05.003.

# Somatic cell encystment promotes abscission in germline stem cells following a regulated block in cytokinesis

**Kari F. Lenhart** and **Stephen DiNardo**

Department of Cell and Developmental Biology; University of Pennsylvania; Philadelphia, PA 19104-6058; USA

Stephen DiNardo: sdinardo@mail.med.upenn.edu

## SUMMARY

In many tissues the stem cell niche must coordinate behavior across multiple stem cell lineages. How this is achieved is largely unknown. We have identified delayed completion of cytokinesis in germline stem cells (GSCs) as a mechanism that regulates the production of stem cell daughters in the *Drosophila* testis. Through live imaging, we show that a secondary F-actin ring is formed through regulation of Cofilin activity to block cytokinesis progress after contractile ring disassembly. The duration of this block is controlled by Aurora B kinase. Additionally, we have identified a requirement for somatic cell encystment of the germline in promoting GSC abscission. We suggest that this non-autonomous role promotes coordination between stem cell lineages. These findings reveal the mechanisms by which cytokinesis is inhibited and reinitiated in GSCs and why such complex regulation exists within the stem cell niche.

## Abstract

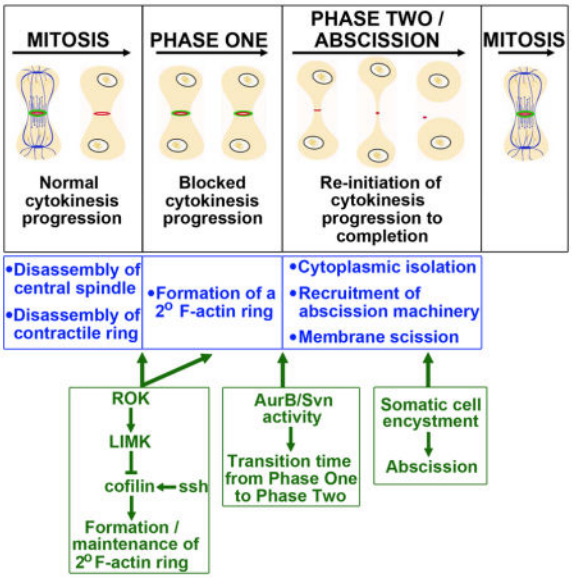


## INTRODUCTION

Stem cells are critical components of many adult tissues. The balance between their self-renewal versus their production of differentiating daughter cells is critical to maintain proper organ homeostasis in the absence of tumor formation. The specialized microenvironment, or niche, surrounding stem cells has emerged as a primary source of multifaceted regulation over stem cell behavior. The niche provides self-renewing signals required to maintain active stem cell populations while often simultaneously controlling the frequency and timing of stem cell divisions. Niche function is particularly complex in tissues in which divisions of multiple stem cell populations must be individually controlled as well as jointly coordinated. In the hematopoietic stem cell (HSC) niche, progeny of the mesenchymal stem cells are thought to contribute to the niche itself and regulate HSC proliferation (Mendelson and Frenette, 2014). Thus, the divisions of one stem cell type are necessary to generate the HSC niche as well as to control daughter cell production in another stem cell lineage. An even greater degree of coordination is required for proper maintenance of mammalian hair follicles. The melanocyte stem cells (MSCs), important for generating pigmentation, and the hair follicle stem cells (HFSCs) critical for continual hair growth, are intermingled at the base of the hair follicle (Blanpain and Fuchs, 2009). During each growth phase, divisions of the HFSCs and MSCs must be tightly coordinated to ensure that pigment is provided to the HFSC progeny cells but not the HFSCs themselves. Disregulation of this division and differentiation pattern has disastrous consequences for the tissue. Pigment uptake by HFSCs induces apoptosis, leading to dramatically increased proliferation rates in the normally slow cycling, remaining HFSCs (Chang et al., 2013). However, while stem cell coordination is obviously critical for proper hair growth, the precise niche-dependent mechanisms controlling this process are not well understood.

The *Drosophila* testis combines features of both the hematopoietic and hair follicle stem cell niches. Just as with HSCs, one population of stem cells in the testis relies upon another for

proper maintenance and self-renewal. The somatic cyst stem cells (CySCs) serve as a component of the niche for the germline stem cells (GSCs). In fact, it is a combination of signals derived from the terminally differentiated hub cells to which CySCs and GSCs are adhered and the CySCs themselves that are necessary for GSC maintenance ((de Cuevas and Matunis, 2011)(Leatherman and DiNardo, 2008) (Leatherman and Dinardo, 2010); Fig. 1A). Similar to regulation in the hair follicle niche, the generation of daughter cells by GSCs and CySCs in the testis must be tightly controlled. Specifically, two somatic cyst cells must be generated by the CySC population for every one differentiating GSC daughter, or gonialblast (Gb) produced ((Tran et al., 2000)(Kiger et al., 2000)). This 2:1 soma to germline ratio is absolutely required for robust germ cell differentiation. As germ cells undergo transit-amplifying divisions characterized by incomplete cytokinesis, they are completely surrounded, or encysted, by their two accompanying cyst cells (Fig. 1A). Disruption of cyst cell-gonial cell interactions blocks differentiation of the germline, much as dysregulating the production of MSC and HFSC daughter cells prevents proper growth of the hair follicle. Importantly, loss of even a single cyst cell from a spermatogonial cyst is sufficient to prevent proper sperm production (Sarkar et al., 2007). As cyst cells do not divide and instead achieve encystment of the germline through extensive cytoskeletal and membrane remodeling, the essential 2:1 ratio of soma to germline must be established within the niche before the Gb moves away from the CySC population required to generate its cyst cell partners.

The complexity of interactions between stem cell lineages in the testis, combined with the stereotyped positioning of the hub, CySCs and GSCs, makes this an ideal system in which to study synchronization of stem cell behavior by the niche. Our analyses revealed that GSC and CySC coordination is not achieved through synchronized cell divisions. Instead, we found that an unusual aspect of GSC cell biology, the extremely delayed completion of cytokinesis between GSC-Gb pairs, likely serves to coordinate the interaction between CySC and GSC daughter cells. By utilizing extended live imaging of GSCs from mitosis through abscission we have clarified the mechanisms controlling delayed cytokinesis in these cells and identified a role for CySCs and cyst cells in regulating this process. We find that GSCs progress through two distinct phases of cytokinesis delay and that these phases are unique to the stem cell population and not observed in differentiating gonia. In addition, we have uncovered three modifications to the traditional cytokinesis program that mediate, respectively, the block, the reinitiation and the completion of GSC-Gb abscission. Excitingly, one of these modifications is a non-autonomous requirement for somatic cell encystment to promote GSC abscission and release of the Gb daughter from the niche. These results provide significant insight into modifications of a fundamental cell biological process required for proper functioning of the testis and reveal a unique mechanism for coordination between stem cell populations in the niche.

# RESULTS

## Coordinated production of stem cell daughters is not achieved through cell cycle synchrony

Once germ cells leave the niche, their differentiation is dependent upon interaction with two somatic cyst cells ((Tran et al., 2000)(Kiger et al., 2000)(Shields et al., 2014)). It has been suggested that synchronized division of a GSC with its flanking CySCs mediates this coordinated production of these three daughter cells (Parrott et al., 2012). However, we found that GSCs and CySCs do not progress synchronously through the cell cycle (Fig. 1B–D3). While many GSCs exhibited partial or complete S phase synchrony with nearby CySCs, 25% completely lacked S Phase coordination (n=32 GSCs; Fig. 1B–B″, D1–D3). Even among the 40% of cases with potential synchrony, nuclear S Phase marking cannot establish whether both S Phase CySCs were indeed encysting the same S Phase GSC. Thus, stringent S phase synchrony does not appear to exist. Consistent with this, we found no evidence of coordinated M phases between the two stem cell populations, as 90% of GSCs entered M phase independently of any flanking CySC (*n*=29 GSCs; Fig. 1C–C″, D1–D3). Therefore, despite the requirement for coordinated daughter cell production, robust synchronization of the cell cycle is not observed between the GSC and CySC stem cell populations.

## GSC cytokinesis is delayed in two phases

Cytokinesis in GSCs is known to be substantially delayed. In fixed tissue, most GSCs are attached to their daughter cells through intercellular (IC) bridges (Hardy et al., 1979). In addition, pulse-chase analysis determined that GSCs remain attached to their daughter Gbs through their next S phase and that GSC-Gb abscission does not occur until G2 of the following cycle (Sheng and Matunis, 2011). We hypothesized that this significant delay in completion of cytokinesis might help coordinate production of stem cell daughters. The delay would ensure that the Gb daughter is retained at the hub, awaiting proper association with two cyst cells before abscission is triggered to release the three cell-grouping from the niche. To address this possibility, we first had to investigate how the delay is established as very little is known about the regulation of cytokinesis in GSCs other than a newly identified role for Aurora B activity in the *Drosophila* ovary (Mathieu et al., 2013).

To characterize the dynamics of GSC-Gb cytokinesis, we conducted live-imaging in testes tracking GSCs from mitosis through abscission using two markers for the IC bridge between GSC-Gb pairs: germ cell expression of the actin binding domain of *moesin* fused to GFP (ABDmoe-GFP) and a ubiquitously expressed myosin regulatory light chain fused to mCherry (Myo-mCherry; Fig. 1E1–E6, MovieS1). We calculated a cell cycle time of about 14 hours (hrs) from the GSCs that underwent two rounds of division during imaging, (n=12; Fig 1F4). We followed 23 GSCs from mitosis through cytokinesis and found that abscission occurred about 12–13 hrs after division (Fig. 1E6, F3). As a GSC entered M-phase, it adopted an elongated shape, with enriched cortical F-actin (Fig. 1E1, MovieS1). After cleavage furrow ingression, the IC bridge was marked for an extended time by an actomyosin ring (Fig. 1E2, E3). F-actin was then lost over a period of 30 min, with the bridge continuing to be marked by a MyoII-labeled midbody ring (Fig. 1E4). The ring

condensed to a midbody as the bridge progressively elongated (Fig. 1E5). Finally, abscission occurred, displacing the daughter Gb away from the hub along with the midbody remnant (Fig. E6, arrow; (Salzmann et al., 2014)). Thus delayed cytokinesis in GSCs could be split into two phases. During Phase One, which averaged about 8.5 hrs, GSC-Gb pairs were attached by an acto-myosin ring (Fig. 1F1). Depolymerization of the F-actin marked entry to Phase Two, during which the IC bridge elongated, the midbody condensed and abscission occurred (Fig. 1F2). Cells only abscised during Phase Two, after disassembly of the F-actin ring.

## Cytokinesis reinitiates during Phase Two

We next analyzed the specific steps of cytokinesis affected that might cause this delay. Since membrane scission occurred at the end of Phase Two, we first determined when abscission machinery was delivered to the intercellular bridge. Normally, the ESCRTIII protein Shrub/Snf7 is trafficked to the IC bridge at the end of mitosis ((Chen et al., 2012)(Lumb et al., 2012)). However, time-lapse analysis of GFP-Shrub showed that its delivery was delayed, remaining diffuse in the cytoplasm through the end of mitosis and into interphase (Fig. 2A1–A3′, MovieS2). Only later did Shrub-GFP puncta move to the IC bridge (Fig. A4, A4′, arrows, MovieS2) where it robustly accumulated about 9.5 hrs following mitosis. Shrub then remained tightly associated with the midbody through abscission (n=7, Fig. 2A4–A5′, MovieS2). Thus, ESCRTIII complex delivery is delayed, only localizing to the IC bridge at the transition to or during Phase Two.

We next tested when cytoplasmic isolation occurs by photo-activating GFP-Tubulin (Tub) in a GSC during Phase One or Phase Two and observing whether or not the signal dispersed into the Gb daughter. Myo-mCherry was used to distinguish Phase One pairs, which had a “midbody ring,” from Phase two, which had a compacted “midbody dot”. As positive and negative controls we activated GFP in one cell of a two-cell cyst (where cells share cytoplasm through a ring canal) or in a GSC that was unattached to a daughter (Fig 2. B–B5′, Movie S3). GFP fluorescence was visible immediately upon photoactivation, and as expected remained restricted to the isolated GSC while rapidly diffusing into the untargeted cell of the 2-cell cyst (highest fractional increase in fluorescence intensity averaged 0.52; Fig. 2B3, B3′ arrow, Movie S3). When one cell of a Phase One pair was activated, we observed rapid diffusion (5/5 pairs) similar to that observed in two-cell cysts (highest fractional increase in fluorescence intensity averaged 0.29; Fig. 2C–C5′, arrows, MovieS4). By contrast, when one cell of a Phase Two pair was activated, we never observed significant signal diffusion between the cells (5/5 pairs; highest fractional increase in fluorescence intensity averaged 0.02; Fig. 2D–D5′, arrow, MovieS5). Taken together, these results show that all steps of abscission occur during Phase Two.

In cells with normal abscission timing, ESCRTIII components are trafficked to the IC bridge along the central spindle, which forms during anaphase and is maintained until just prior to abscission ((Chen et al., 2012) (Lumb et al., 2012)). The late arrival of Shrub-GFP could suggest an aberrantly long persistence of the central spindle in GSCs. Surprisingly, live-imaging of tubulin-GFP showed approximately normal kinetics of central spindle dissolution. Mitotic GSCs were identified by the accumulation of tubulin-GFP at

centrosomes (Fig. 2E, arrows, MovieS6). A metaphase spindle was formed within about 10 min followed immediately by furrow ingression and formation of a compact central spindle (Fig. 2E1–E2, arrows, MovieS4). Microtubule enrichment then decreased at the central spindle and was no longer detected by about 2.3 hrs after first appearance (Fig. 2E1–E5, arrows, MovieS6). We confirmed that the central spindle was dissolved prior to Phase Two by immunofluorescent staining of β-tubulin in fixed cells. Indeed, 66% of attached GSC-Gb pairs contained no evidence of a central spindle (n=42; Fig. 2F–F″). Importantly, pairs with a detectable central spindle were all in Phase One, as judged by the presence of an F-actin ring (n=23; Fig. 2G–G″, arrowheads). Thus, the central spindle is disassembled early in Phase One and is absent prior to recruitment of abscission machinery in Phase Two. Taken together, the results show that cytokinesis in GSCs progresses normally through furrow ingression and central spindle disassembly. Cytokinesis is then blocked during Phase One and does not reinitiate until cytoplasmic isolation occurs at the onset of or during Phase Two.

## A secondary F-actin ring blocks cytokinesis

Given the block to cytokinesis in Phase One, we focused next on the F-actin ring. The actin-myosin contractile ring is critically required for furrow ingression, but this structure must be disassembled for abscission to occur ((Pollard, 2010)(Kaji et al., 2003)). We imaged F-actin and myosin with shorter time intervals to definitively establish whether abscission was blocked due to persistence of the contractile ring. GSCs entering M-Phase were identified by cortical enrichment of F-actin (Fig. 3A1, A1′). The furrow ingressed through anaphase and telophase, ending with an actomyosin ring diameter averaging 1.2um (Fig. 3A1–A3′, arrowheads). Shortly thereafter, the F-actin component of the contractile ring began to depolymerize (Fig. 3A4, A4′, arrowheads) with complete disassembly in the majority of cells (44/47). In contrast, the myo-mCherry-labeled midbody ring was retained (Fig. 3A5, A5′, arrowheads). Thus, contractile ring F-actin is disassembled at the end of mitosis just as would occur in cells that abscise without a delay. However, instead of proceeding toward abscission, over the next 30 minutes there were bursts of actin polymerization with small foci appearing on either side of the Myo-mCherry-labeled midbody ring or on the GSC or Gb cell cortex adjacent to the IC bridge (Fig. 3A6, A6′, arrows). Ultimately, these foci resolved into a new F-actin ring (Fig. 3A7, A7′, arrowheads) that would persist for many hours through Phase One (Fig S1A1–A5″). Thus, this secondary ring is a candidate for the block in cytokinesis progression.

## Cofilin activity controls cytokinesis progress by regulating the secondary F-actin ring

As the secondary ring is established within an hour of contractile ring disassembly, we asked whether manipulation of factors required for actin depolymerization at the contractile ring might also influence secondary ring formation. The actin severing protein Cofilin is required for contractile ring disassembly, and Cofilin activity is exquisitely regulated throughout mitotic progression. Activity is inhibited during early stages by LIM Kinase (LimK), and activated during late cytokinesis by a combination of decreased LimK activity and increased de-phosphorylation by the phosphatase Slingshot (Ssh) ((Amano et al., 2002)(Kaji et al., 2003)). The extant loss-of-function *cofilin* alleles were not useful, being either too weak, and exhibiting no effects on actin dynamics, or too strong, and causing loss of the GSCs (data

not shown). However, we speculated that formation of the secondary F-actin ring might require inhibition of the high Cofilin activity normally established during late cytokinesis. If this were the case, then forcing high Cofilin activity might destabilize the secondary ring. We tested this by expressing either the activating phosphatase Ssh or a constitutively active (CA) Cofilin in germ cells (Fig. 4B1–C4). In 2 of 37 pairs, the secondary F-actin ring completely failed to form, with cells transitioning directly from mitosis into Phase Two. In the other pairs, the secondary F-actin ring formed, but its lifetime was significantly shortened by on average 3 hrs compared to controls (Fig 4F1; Table S1). Importantly, in those GSCs with a shorter Phase One, abscission occurred 2–3 hours earlier than controls (Fig. 4F3; Table S1).

To confirm these results, we also manipulated Cofilin function by analyzing testes deficient for LimK, which inhibits Cofilin by phosphorylation, and testes treated with a pharmacological inhibitor of Rho Kinase (ROK), which activates LimK (Fig. 4D1–E4). We found that both conditions led to more rapid loss of the secondary ring and thus a shorter Phase One (Fig. 4F1; Table S1). Again, precocious exit from Phase One led to earlier abscission of GSC-Gb pairs (2.5 hours upon LimK or ROK loss-of-function; Fig. 4F1–F3; Table S1). Notably in all these manipulations, the length of Phase Two remained similar to controls, indicating that the steps necessary for abscission were not speeded up. Thus, we conclude that an F-actin structure, distinct from the contractile ring, is generated at the end of mitosis, likely through alterations in Cofilin activity, and this structure blocks the progress of cytokinesis. Ultimately, this block delays the initiation of abscission until Phase Two.

## Aurora B regulates the length of cytokinesis delay

We next addressed the regulation of Phase Two, noting that Aurora B (AurB) and Survivin (Svn), essential components of the chromosomal passenger complex (CPC), can block abscission in Drosophila ovarian GSCs and early germ cells, or in cultured cells when there are defects in chromosome segregation ((Steigemann et al., 2009)(Mathieu et al., 2013)). In particular, persistent Svn activity delays abscission in female GSCs. To test if AurB/Svn activity could similarly inhibit abscission in the testis, we imaged male GSCs expressing a form of Survivin that mimics its phosphorylation by AurB regulation and acts as gain-of-function (*nos*>SvnS125E) (Mathieu et al., 2013). Indeed, Phase Two was consistently longer in these GSC-Gb pairs (6.5 hrs versus 4.5 hrs in controls; Fig. 5B1–B6, D2; Table S2). However, the majority of pairs abscised (Fig. 5D4; Table S2), in contrast to the case in female GSCs. Thus, persistent CPC activity at the IC bridge delayed but did not block abscission.

Additionally, we uncovered a surprising role for AurB/Svn activity in regulating the timing of the Phases One-Phase Two transition. Phase One was substantially shorter with SvnS125E (5 hrs versus 8.5 hrs; Fig. 5D1; Table S2). Reciprocally, Phase One was significantly longer in GSC-Gb pairs depleted for *aurb* (Fig. 5C1–C6, D1; 9.5 hrs versus 8.5 hrs; Table S2). Therefore, both gain- and loss-of-function implicate AurB/Svn in the transition between Phase One and Two. Interestingly, the time from division to division in $aurb^{1689}$ was unchanged (Fig. 5D5; Table S2). Since more time was spent in Phase One,

*aurB* mutant GSC-Gb pairs spent a higher proportion of their cell cycle with abscission progress blocked than did controls (75% versus 60%, respectively). This delay in the transition between Phases One and Two consistently led to an inability of pairs to abscise prior to the next mitosis, resulting in the formation of 4-cell cysts attached to the hub (Fig. 5C5, C6). Note that GSC remained anchored to the hub, and its second division was still oriented away from the hub strongly suggesting that depletion of *aurb* did not affect stem cell fate.

Thus, CPC activity plays a unique role during the modified cytokinesis in GSCs. The complex *promotes* the completion of cytokinesis by regulating timing of the transition between Phase One (blocked abscission) and Phase Two (abscission progress) and is required for proper release of differentiating daughter cells.

## Delayed GSC abscission is distinct from incomplete cytokinesis of gonial cysts

A complete block during cytokinesis is a feature of differentiating germ cells in most animals ((FAWCETT et al., 1959)(Spradling et al., 2011). Thus, we asked whether the delayed abscission of GSCs was simply related to that feature or represented a unique program imposed specifically on the GSCs. We examined mitosis in two cell cysts to test whether the contractile F-actin was disassembled and a secondary F-actin ring formed, as in GSCs. Acto-myosin contractile rings were visible immediately following anaphase at the nascent IC bridges between new differentiating daughter cells (Fig. 6A, A1 blue arrowheads). However, F-actin was never lost from the IC bridges between differentiating gonia ($n$=15/15; Fig. 6A1–A5). Thus, the contractile ring F-actin is maintained with no evidence for the secondary actin ring found in GSCs. Consistent with this, we found that maintenance of ring canal F-actin in the differentiating germ cells was not mediated by control of Cofilin activity since disrupting LimK or ROK function had largely no effect in two cell cysts (14/16 cysts with ROK inhibition, 12/12 cysts in $LimK^{2}$; Fig. 6B–C5). We conclude that Phase One is imposed specifically on GSCs.

Further evidence that cytokinesis is regulated uniquely in male GSCs derives from our analysis of AurB function. In the ovary, AurB activity delays abscission in GSCs and blocks inappropriate abscission in differentiating cells (Mathieu et al). In contrast, in male GSCs AurB promoted the progression to abscission (Fig 5. D1), and our analysis revealed no significant role for AurB in differentiating germ cells. Specifically, live imaging of Gb divisions revealed the maintenance of F-actin at ring canals between nascent daughter cells immediately following mitosis ($n$=7/7; Fig. 6D–D2) and, importantly, these ring canals remained intact for the duration of imaging (Fig. 6D2–D5). Thus, delayed cytokinesis is regulated uniquely in male GSCs, and is mechanistically distinct from incomplete cytokinesis in differentiating gonia.

## Somatic cell encystment is required for abscission

Having developed the tools to characterize GSC abscission, we could now address whether the coordinated production of germline and somatic stem cell daughters involved control over this process. Specifically, we asked whether encystment by somatic cells regulates GSC abscission. Encystment is mediated by EGF receptor (EGFR) activation in somatic

cells ((Chen et al., 2013; Kiger et al., 2000; Sarkar et al., 2007; Tran et al., 2000)). To disrupt this, we expressed dominant-negative EGFR in CySCs and cyst cells (*c587*>egfr$^{DN}$). In these testes GSCs progressed normally through Phases One and Two of delay, similar to driver-only controls (Fig. 7A1–B4). Interestingly, rather than completing abscission, most GSC-Gb pairs entered a second round of mitosis while still attached, generating four interconnected germ cells adhered to the hub (Fig. 7B5, B6, MovieS7). In most cases, the four-cell groupings remained at the hub for the duration of our imaging (Fig. 7B6). However, in rare examples, the entire set of cells was released from the hub as a four-cell cyst or one of the IC bridges was resolved, leading to release of two or three interconnected cells (data not shown).

EGF signaling promotes encystment by acting through Rac to alter the actin cytoskeleton and membrane architecture of the somatic cells (Sarkar et al., 2007). Indeed, we found that disrupting actin dynamics (Fig. S3B–B5) or expressing a dominant-negative form of Rac within the CySCs and cyst cells blocked abscission in many GSCs (Fig 7C1–C4). GSC-Gb pairs entered a second round of mitosis while still attached (Fig. 7C2), with the resultant four germ cells remaining interconnected and attached to the hub for an extended period (Fig. 7 C3, C4). Strikingly, three GSC-Gb pairs in testes with somatic expression of Rac1$^{DN}$ underwent a second division without physically separating, resulting in eight interconnected cells remaining associated with the hub (Fig. S3A–A5). Of the 32 attached divisions we observed, only 8 resulted in the eventual release of any GSC daughters from the niche. Thus, somatic cell encystment of the germline is required to promote abscission between GSC-Gb pairs.

We next addressed whether loss of abscission had a consequence on cell fate, by testing whether the interconnected cells exhibited stem cell or differentiating cell behavior. As already noted, we consistently observed continued attachment to the hub by one cell of the cyst and appropriately oriented divisions of the GSC-Gb pair, as would be expected of stem cells. However, the 4-cell clusters consistently contained branched fusomes (Fig. 7C5; $n$=10), a structure normally spherical or bar-shaped in stem cells and branched only in differentiating cells (de Cuevas and Spradling, 1998). Additionally, following attached divisions of GSC-Gb pairs, we found that only the germ cell adherent to the hub and its immediate daughter were enriched for Stat protein (Fig. 7D–E″ “GSC-pair”). Stat accumulation, though not critical for GSC renewal, is nonetheless a hallmark of the stem cell populations within the testis (Leatherman and Dinardo, 2010), and thus suggested mixed character of the interconnected cells. Finally, we analyzed whether secondary F-actin rings, a feature we have shown is specific to the stem cell, formed as the abscission-blocked GSC-Gb pairs generated a 4-cell cyst. Time lapse imaging in testes with somatic expression of Rac1$^{DN}$ demonstrated that the contractile ring F-actin was disassembled at all IC bridges among the four cells ($n$=7/7; Fig. 7D–D4′, blue arrowheads). Subsequently, a secondary F-actin ring assembled at all bridges, similar to normal GSC divisions (Fig. 7D5–D5′). We thus conclude that when abscission is blocked in GSC-Gb pairs the cells exhibit mixed characteristics of stem and differentiating cells, a feature profoundly detrimental to both the production of differentiating germ cells and the maintenance of a robust stem cell population in the testis.

## DISCUSSION

This first real-time analysis of GSCs through abscission has revealed surprising complexities layered in cytokinesis (Fig. S3). First, cytokinesis is blocked after central spindle and contractile ring disassembly and before entry to the abscission phase. This block is imposed by a secondary F-actin-ring. Second, in a role AurB regulates the transition between Phase One and Two. That transition marks a vital step in the reinitiation of cytokinesis, permitting cytoplasmic isolation and recruitment of abscission machinery. Finally, somatic cell encystment is essential to abscission. Thus, three discrete nodes of regulation are layered on top of the canonical cytokinesis program to achieve tight temporal control over daughter cell production, and thus tissue maintenance by the resident stem cells.

### Stem cell specificity in cytokinesis delay

Incomplete cytokinesis is a deeply conserved feature of germ cells that establishes the syncytium necessary for robust germ line development ((FAWCETT et al., 1959; Spradling et al., 2011)). Differentiating germ cells appear to arrest cytokinesis immediately following contractile ring ingression, since the known components of stable ring canals are identical to those of the contractile ring (Hime et al., 1996). It was thought that delayed cytokinesis in GSCs was simply a remnant of this conserved program. In contrast we found that the delay is mechanistically distinct from that occurring in differentiating germ cells. GSCs complete ingression, disassemble their contractile ring F-actin and dissolve central spindle microtubules before engaging a ROK-LimK-Cofilin pathway to regulate a secondary F-actin ring that blocks cytokinesis progression until its disassembly at the entry to Phase Two.

Interestingly, the F-actin rings of gonial cells were not disrupted by manipulation of Cofilin activity, in contrast to their precocious disassembly in GSC-Gb pairs. This functional distinction is likely tied to the different biological goal of the stem cell versus the differentiating germ cell. One must release a differentiating daughter cell while the other must communicate syncitially for differentiation to progress normally. Ultimately, since the stem cell niche confers this functional distinction, future work will investigate whether it directly controls F-actin dynamics in the stem cell by possibly modulating Cofilin, or acts indirectly through other stem cell factors to do so.

### The secondary F-actin ring blocks progress toward abscission

Our data strongly indicates that the secondary F-actin ring must be disassembled in order for abscission to be reinitiated. This suggests that F-actin at the IC bridge inhibits abscission, and work in other cells supports this. Inhibition of the Cofilin phosphatase, activation of AurB, depletion of phosphoinositide 5-phosphatase or of Rab35 all lead to retention of F-actin at the IC bridge and inhibited abscission ((Dambournet et al., 2011; Kaji et al., 2003; Steigemann et al., 2009)). Importantly, abscission could be restored after Rab35 depletion by forcing F-actin disassembly (Dambournet et al., 2011).

## CPC activity ensures abscission prior to mitosis by regulating the Phase One transition to Phase Two

GSC-Gb pairs depleted for *aurB* fail to complete abscission prior to mitotic entry and form interconnected germ cells attached to the hub. This could suggest that AurB is normally required to promote abscission. However, expressing an activated form of Svn did not induce precocious abscission as would be expected in this model. Rather, SvnS125E expression advanced the transition from Phase One to Two, while *aurB* depletion delayed it (Fig. 6S–U). These reciprocal effects suggest instead that AurB times the Phase One-Phase Two transition. In this model, the lack of abscission in *aurB* mutants is an indirect consequence of spending a shorter fraction of the total cycle in Phase Two. For example, we have shown that ESCRTIII is localized during Phase Two and in the apparent absence of central spindle microtubules. In *aurb* depleted cells, there simply may not be enough time during the shortened Phase Two for the already compromised recruitment of ESCRTIII machinery to promote abscission prior to mitotic entry. We note also that the lack of a central spindle raises the issue of how ESCRTIII components are delivered to the IC bridge. Perhaps the midbody performs this role, as has been suggested for the *C. elegans* first cell division (Green et al., 2013).

Recent studies have found that shrub is negatively regulated by AurB in female GSCs (Matias et al., 2015). Though our results suggest that AurB activity should promote ESCRTIII function in the testis, it is compelling to speculate that AurB might control the Phase One-Phase Two transition through shrub. Alternatively, AurB could directly control this transition by regulating disassembly of the secondary F-actin ring, as there is precedent for AurB controlling actin dynamics. For example, in the “No Cut” pathway maintenance of AurB activity late in cytokinesis is associated with persistence of F-actin at the IC bridge (Steigemann et al., 2009). Intriguingly, AurB can phosphorylate formin proteins and thereby regulate actin stress fiber formation ((Cheng et al., 2011b; Floyd et al., 2013; Ozlü et al., 2010)). Although in this context AurB activity positively regulates actin polymerization, the interaction between AurB and formin suggests a direct link between CPC activity and actin dynamics. This connection is particularly compelling given that formins can also promote severing of actin filaments (Bohnert et al., 2013). Thus, it is intriguing to speculate that AurB phosphorylation of formins at the IC bridge in GSC-Gb pairs may promote severing of actin filaments in the secondary ring and thereby promote transition from Phase One to Phase Two of delay.

## Somatic cell encystment promotes GSC-Gb abscission

Perhaps most excitingly, we have identified non-autonomous control over GSC-Gb abscission by somatic cell encystment. We believe this sheds light on the functional relevance of abscission delay. Encystment of spermatogonia by two somatic cells is required for proper germ cell differentiation ((Kiger et al., 2000; Sarkar et al., 2007; Tran et al., 2000)). However, we found that GSCs and their flanking CySCs do not coordinate daughter cell production by synchronizing their cell cycles. Linking abscission to encystment is an elegant alternative for promoting coordinated release of stem cell daughters from the niche.

Several questions are raised by our observations, such as precisely when abscission is triggered relative to cyst cell engulfment of the Gb. It would be necessary to carry out live-imaging simultaneously on germline and adjacent somatic cells to address this. However, imaging CySCs and cyst cells is fraught with difficulty due to their irregular morphology and small size (see discussion in (Cheng et al., 2011a)). Thus, we have not yet been able to image somatic cells with anywhere near the resolution achieved for GSC-Gb pairs (K. Lenhart, unpublished data).

Encystment could promote abscission through contact-dependent signaling, where CySCs or cyst cells produce the ligand. Alternatively, the abscission trigger might be mechanical, since tension has been suggested to regulate abscission in cultured cells. Here, as daughter cells migrated apart in culture following mitosis, tension along the bridge connecting them increased and this lengthened the time to abscission (Lafaurie-Janvore et al., 2013). Experimentally decreasing bridge tension triggered earlier abscission (Lafaurie-Janvore et al., 2013). In our system, most Gbs are displaced some distance from the hub during Phase Two, with a consequent elongation of the IC bridge connecting those cells to the GSC (Fig. 1H, I). Perhaps movement of the Gb away from its mother GSC generates increased tension along the bridge. Symmetric encystment might relieve that tension by providing equalizing forces on both sides of the IC bridge, inducing abscission while ensuring that the Gb is properly associated with two somatic cells. Since in culture increased tension delayed abscission by disrupting assembly of functional ESCRTIII complexes at the IC bridge (Lafaurie-Janvore et al., 2013), in GSCs it will be interesting to address whether ESCRTIII complexes are temporally regulated by encystment. Whatever the mechanism, the cyst cells are clearly poised for intimate contact at the appropriate time, as the midbody remnant is sometimes taken up by encysting somatic cells after abscission (Salzmann et al., 2014).

This work has clarified the mechanism by which cytokinesis is delayed in GSCs, identifying three distinct regulatory events layered on top of the traditional program of cytokinesis. These events impose an appropriate delay, a timed reinitiation and a regulated abscission in the GSCs. This stem cell-specific program assists in the coordinate release of differentiating daughter cells from the resident stem cell populations in this niche. Since similar requirements for synchronized daughter cell production between multiple stem cell populations exist in other tissues, it is enticing to speculate that regulated abscission might be used to promote coordination in other niches. Membrane scission is difficult to visualize *in vivo* in many systems, so it is not yet known if stem cells other than the germline exhibit abscission delay. As higher resolution methods are developed to visualize stem cell dynamics within endogenous niches, it will be interesting to see if abscission delay emerges as a conserved mechanism of niche-dependent control over stem cell proliferation.

## EXPERIMENTAL PROCEDURES

### Fly Stocks and Crosses

Traffic Jam Gal4 (Kyoto Stock Center), *c587* Gal4 (Erika Matunis), *nos* Gal4-VP16 (Ruth Lehmann and Erica Selva), ABD-moeGFP under the *nanos* germ cell promoter (Sano, 2005), $LimK^{2}$ (Huey Hing (Ang et al., 2006)) $sqh^{P}$-*sqh*::$mCherry^{A11}$ (Adam Martin (Martin et al., 2009)), $aurB^{1689}$ and UAS-SvnS12 5E (Jean-René Huynh (Mathieu et al., 2013)) and

UAS-egfr$^{DN}$ (Trudi Schupbach). All remaining stocks: UAS-Ssh, UAS-tsr$^{S3A}$, UAS-ShrubGFP, UAS-Rac1.N17 and UAS-PA-TubGFP were from the Bloomington Stock Center. For experiments addressing encystment, flies expressing GAL80$^{ts}$ (Bloomington) and *c587* alone, *c587*>egfr$^{DN}$ or *tj*>rac1$^{DN}$ were grown at 18°. Newly eclosed males were transferred to 29° and kept at this temperature for 3–4 days until encystment phenotype developed.

## Time Lapse Imaging

The protocol for culture conditions was modified from (Sheng and Matunis, 2011). Testes were dissected from newly eclosed males in Ringers solution and transferred to a poly-lysine-coated coverslip bottom of a round imaging dish (MatTek). Ringers was removed and imaging media (15% FBS, 0.5X penicillin/streptomycin, 0.2 mg/mL insulin in Schneider's insect media) was added. For ROK inhibitor experiments, the imaging media additionally contained 380μM of the Y-27632 drug. Testes were imaged on either a Leica DM16000 B inverted spinning disk confocal or an Olympus IX71 inverted spinning disk confocal overnight for up to 19 hrs. Our time lapse analyses of wild type testes revealed low frequencies of symmetric renewals and symmetric losses, as previously reported ((Sheng and Matunis, 2011). For all imaging, 43 micron stacks were acquired with a Z step size of one micron using a 63x/1.2 NA lens (on the Leica system) or a 60x/1.2 NA lens (on the Olympus system). Analysis was performed on the full 4D series and 2–14 Z planes were selected and Z projections generated for figure panels. Unless otherwise indicated, images were collected at 25 min intervals and times reported in figure panels have been rounded to the nearest half hour. Separate GSC-Gb pairs were followed for timing analyses reported in Fig. 1 and Fig. 4. The same pairs were followed for the entire analysis reported in Fig. 5. We note that previous studies have suggested a longer cycling time for GSCs than what we have determined. We believe this derives from a combination of factors. First, our analysis is the only one that has determined the GSC cycling rate by directly visualizing two rounds of GSC mitoses. Second, we are reporting a cycling rate from those GSCs that divided twice during our imaging period. This might underestimate the rate over the whole population of GSCs, as the GSC cell cycles that we reported necessarily had periods of less than 18 hours.

## Immunostaining and S-Phase Labeling

Immunostaining was performed as previously described (Terry et al., 2006). Antibodies used: goat anti-vasa (Santa Cruz, 1:250), guinea pig anti-traffic jam (Dorothea Godt, 1:10,000), chick anti-GFP (1:10,000), rabbit anti-phospho-histone H3 (1:50,000), rabbit anti-Stat (Erika Bach) and mouse anti-fasciclin 3 (Developmental Studies Hybridoma Bank [DSHB], 1:500). S-Phase labeling was performed as previously described (Leatherman and Dinardo, 2010).

## Image and Statistical Analysis

Time lapse images were analyzed and Z projections generated using Fiji software. Student T-tests were used for all statistical comparisons. In each analysis, p values less than 0.05 were considered to be statistically significant.

### Quantification of Photo-activation

Pixel intensity was determined for converted and unconverted cells at each time point by manually drawing regions of interest in ImageJ. Background intensity was subtracted from each value and the ratio of intensity in the unconverted versus converted cell was determined at each time point. Excel, we used the “Solver” function to perform non-linear curve fitting. The data is reported as the average highest fractional increase, as determined from the non-linear curve fit.

## Supplementary Material

Refer to Web version on PubMed Central for supplementary material.

## Acknowledgments

We thank D. Godt, J.-R. Huynh, H. Hing and T. Schüpbach for antibodies and fly stocks. Thanks to E. Bi, J. Schottenfeld-Roames, Y. Elkouby and members of the DiNardo lab for comments on the manuscript. We thank E. Matunis for advice on live imaging and A. Stoudt and the CDB Microscopy Core for assistance and advice on imaging. Supported by R01 GM60804 (SD) and ACS Post-doctoral Fellowship PF-13-029-01-DDC (K.F.L.).

## References

Amano T, Kaji N, Ohashi K, Mizuno K. Mitosis-specific activation of LIM motif-containing protein kinase and roles of cofilin phosphorylation and dephosphorylation in mitosis. J Biol Chem. 2002; 277:22093–22102. [PubMed: 11925442]

Ang LH, Chen W, Yao Y, Ozawa R, Tao E, Yonekura J, Uemura T, Keshishian H, Hing H. Lim kinase regulates the development of olfactory and neuromuscular synapses. Dev Biol. 2006; 293:178–190. [PubMed: 16529736]

Blanpain C, Fuchs E. Epidermal homeostasis: a balancing act of stem cells in the skin. Nat Rev Mol Cell Biol. 2009; 10:207–217. [PubMed: 19209183]

Bohnert KA, Willet AH, Kovar DR, Gould KL. Formin-based control of the actin cytoskeleton during cytokinesis. Biochem Soc Trans. 2013; 41:1750–1754. [PubMed: 24256286]

Chang CY, Pasolli HA, Giannopoulou EG, Guasch G, Gronostajski RM, Elemento O, Fuchs E. NFIB is a governor of epithelial–melanocyte stem cell behaviour in a shared niche. Nature. 2013; 495:98–102. [PubMed: 23389444]

Chen CT, Hehnly H, Doxsey SJ. Orchestrating vesicle transport, ESCRTs and kinase surveillance during abscission. Nat Rev Mol Cell Biol. 2012; 13:483–488. [PubMed: 22781903]

Chen H, Chen X, Zheng Y. The nuclear lamina regulates germline stem cell niche organization via modulation of EGFR signaling. Cell Stem Cell. 2013; 13:73–86. [PubMed: 23827710]

Cheng J, Tiyaboonchai A, Yamashita YM, Hunt AJ. Asymmetric division of cyst stem cells in Drosophila testis is ensured by anaphase spindle repositioning. Development. 2011a; 138:831–837. [PubMed: 21303845]

Cheng L, Zhang J, Ahmad S, Rozier L, Yu H, Deng H, Mao Y. Aurora B regulates formin mDia3 in achieving metaphase chromosome alignment. Dev Cell. 2011b; 20:342–352. [PubMed: 21397845]

De Cuevas M, Matunis EL. The stem cell niche: lessons from the Drosophila testis. Development. 2011; 138:2861–2869. [PubMed: 21693509]

De Cuevas M, Spradling AC. Morphogenesis of the Drosophila fusome and its implications for oocyte specification. Development. 1998; 125:2781–2789. [PubMed: 9655801]

Dambournet D, Machicoane M, Chesneau L, Sachse M, Rocancourt M, El Marjou A, Formstecher E, Salomon R, Goud B, Echard A. Rab35 GTPase and OCRL phosphatase remodel lipids and F-actin for successful cytokinesis. Nat Cell Biol. 2011; 13:981–988. [PubMed: 21706022]

FAWCETT DW, ITO S, SLAUTTERBACK D. The occurrence of intercellular bridges in groups of cells exhibiting synchronous differentiation. J Biophys Biochem Cytol. 1959; 5:453–460. [PubMed: 13664686]

Floyd S, Whiffin N, Gavilan MP, Kutscheidt S, De Luca M, Marcozzi C, Min M, Watkins J, Chung K, Fackler OT, et al. Spatiotemporal organization of Aurora-B by APC/CCdh1 after mitosis coordinates cell spreading through FHOD1. J Cell Sci. 2013; 126:2845–2856. [PubMed: 23613471]

Green RA, Mayers JR, Wang S, Lewellyn L, Desai A, Audhya A, Oegema K. The midbody ring scaffolds the abscission machinery in the absence of midbody microtubules. J Cell Biol. 2013; 203:505–520. [PubMed: 24217623]

Hardy RW, Tokuyasu KT, Lindsley DL, Garavito M. The germinal proliferation center in the testis of Drosophila melanogaster. J Ultrastruct Res. 1979; 69:180–190. [PubMed: 114676]

Hime GR, Brill JA, Fuller MT. Assembly of ring canals in the male germ line from structural components of the contractile ring. J Cell Sci. 1996; 109(Pt 1):2779–2788. [PubMed: 9013326]

Kaji N, Ohashi K, Shuin M, Niwa R, Uemura T, Mizuno K. Cell cycle-associated changes in Slingshot phosphatase activity and roles in cytokinesis in animal cells. J Biol Chem. 2003; 278:33450–33455. [PubMed: 12807904]

Kiger AA, White-Cooper H, Fuller MT. Somatic support cells restrict germline stem cell self-renewal and promote differentiation. Nature. 2000; 407:750–754. [PubMed: 11048722]

Lafaurie-Janvore J, Maiuri P, Wang I, Pinot M, Manneville JB, Betz T, Balland M, Piel M. ESCRT-III Assembly and Cytokinetic Abscission Are Induced by Tension Release in the Intercellular Bridge. Science (80-). 2013; 339:1625–1629.

Leatherman JL, DiNardo S. Zfh-1 Controls Somatic Stem Cell Self-Renewal in the Drosophila Testis and Nonautonomously Influences Germline Stem Cell Self-Renewal. Cell Stem Cell. 2008; 3:44–54. [PubMed: 18593558]

Leatherman JL, Dinardo S. Germline self-renewal requires cyst stem cells and stat regulates niche adhesion in Drosophila testes. Nat Cell Biol. 2010; 12:806–811. [PubMed: 20622868]

Lumb JH, Connell JW, Allison R, Reid E. The AAA ATPase spastin links microtubule severing to membrane modelling. Biochim Biophys Acta. 2012; 1823:192–197. [PubMed: 21888932]

Martin AC, Kaschube M, Wieschaus EF. Pulsed contractions of an actin-myosin network drive apical constriction. Nature. 2009; 457:495–499. [PubMed: 19029882]

Mathieu J, Cauvin C, Moch C, Radford SJ, Sampaio P, Perdigoto CN, Schweisguth F, Bardin AJ, Sunkel CE, McKim K, et al. Aurora B and cyclin B have opposite effects on the timing of cytokinesis abscission in Drosophila germ cells and in vertebrate somatic cells. Dev Cell. 2013; 26:250–265. [PubMed: 23948252]

Matias NR, Mathieu J, Huynh JR. Abscission Is Regulated by the ESCRT-III Protein Shrub in Drosophila Germline Stem Cells. PLoS Genet. 2015; 11:e1004653. [PubMed: 25647097]

Mendelson A, Frenette PS. Hematopoietic stem cell niche maintenance during homeostasis and regeneration. Nat Med. 2014; 20:833–846. [PubMed: 25100529]

Ozlü N, Monigatti F, Renard BY, Field CM, Steen H, Mitchison TJ, Steen JJ. Binding partner switching on microtubules and aurora-B in the mitosis to cytokinesis transition. Mol Cell Proteomics. 2010; 9:336–350. [PubMed: 19786723]

Parrott BB, Hudson A, Brady R, Schulz C. Control of germline stem cell division frequency--a novel, developmentally regulated role for epidermal growth factor signaling. PLoS One. 2012; 7:e36460. [PubMed: 22586473]

Pollard TD. Mechanics of cytokinesis in eukaryotes. Curr Opin Cell Biol. 2010; 22:50–56. [PubMed: 20031383]

Salzmann V, Chen C, Chiang CYA, Tiyaboonchai A, Mayer M, Yamashita YM. Centrosome-dependent asymmetric inheritance of the midbody ring in Drosophila germline stem cell division. Mol Biol Cell. 2014; 25:267–275. [PubMed: 24227883]

Sano H. Control of lateral migration and germ cell elimination by the Drosophila melanogaster lipid phosphate phosphatases Wunen and Wunen 2. J Cell Biol. 2005; 171:675–683. [PubMed: 16301333]

Sarkar A, Parikh N, Hearn SA, Fuller MT, Tazuke SI, Schulz C. Antagonistic Roles of Rac and Rho in Organizing the Germ Cell Microenvironment. Curr Biol. 2007; 17:1253–1258. [PubMed: 17629483]

Sheng XR, Matunis E. Live imaging of the Drosophila spermatogonial stem cell niche reveals novel mechanisms regulating germline stem cell output. Development. 2011; 138:3367–3376. [PubMed: 21752931]

Shields AR, Spence AC, Yamashita YM, Davies EL, Fuller MT. The actin-binding protein profilin is required for germline stem cell maintenance and germ cell enclosure by somatic cyst cells. Development. 2014; 141:73–82. [PubMed: 24346697]

Spradling A, Fuller MT, Braun RE, Yoshida S. Germline stem cells. Cold Spring Harb Perspect Biol. 2011; 3:a002642. [PubMed: 21791699]

Steigemann P, Wurzenberger C, Schmitz MHA, Held M, Guizetti J, Maar S, Gerlich DW. Aurora B-Mediated Abscission Checkpoint Protects against Tetraploidization. Cell. 2009; 136:473–484. [PubMed: 19203582]

Terry NA, Tulina N, Matunis E, DiNardo S. Novel regulators revealed by profiling Drosophila testis stem cells within their niche. Dev Biol. 2006; 294:246–257. [PubMed: 16616121]

Tran J, Brenner TJ, DiNardo S. Somatic control over the germline stem cell lineage during Drosophila spermatogenesis. Nature. 2000; 407:754–757. [PubMed: 11048723]

## HIGHLIGHTS

- GSCs delay cytokinesis in two distinct phases
- A ROK-LimK-Cofilin pathway regulates Phase One of delay
- Aurora B activity controls the time of transition between Phases One and Two
- Somatic cell encystment promotes GSC abscission

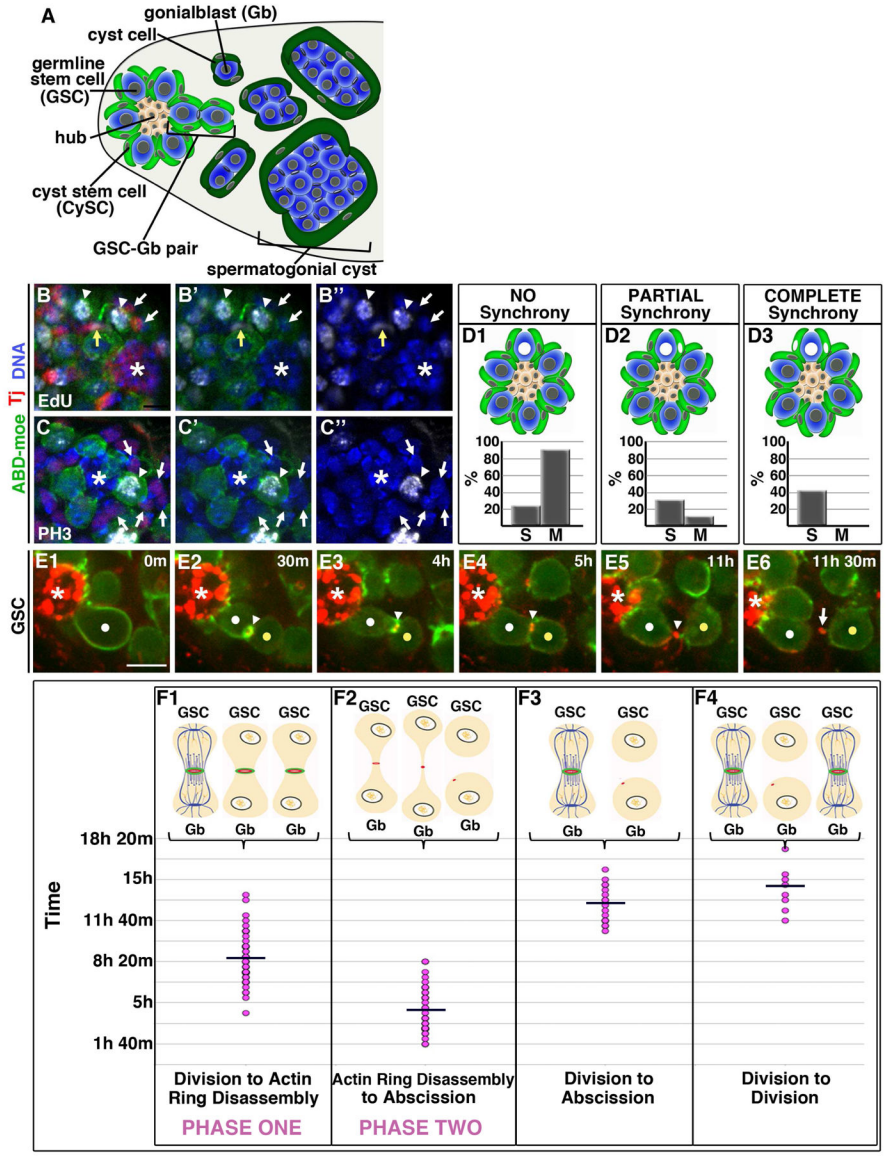


**Figure 1. Two phases of delayed cytokinesis in GSCs**

(A) Diagram of testis niche

(B–C″) Immunofluorescence of 30 min EdU pulse-labeled testes (white, B–B″), or stained with phospho-Histone H3 antibody (PH3; white, C–C″). Tj=Traffic jam (red, somatic cell nuclei). *=Hub. (B–B″) A GSC-Gb pair (arrowheads) in S Phase shows partial synchrony with one adjacent CySC (yellow arrow) while the majority of surrounding somatic nuclei are EdU-negative (white arrows). (C–C″) A GSC in mitosis (arrowhead) exhibiting no synchrony with surrounding CySCs (arrows).

(D1–D3) Quantification of S and M Phase Synchrony

(E1–E6) Time lapse imaging of GSC division cycle; ABD-moeGFP and Myo-mCherry. Each panel is a 3–5 Z plane projection. m=min. h=hour. White dot=GSC. Yellow dot=Gb. Arrowhead=IC bridge. Arrow=midbody remnant. *=Hub. Scale bar=5 microns

(F1–F4) Quantification of timing of indicated phases; each dot=individual GSC-Gb pair. Line=average time.
See also Fig. S2.

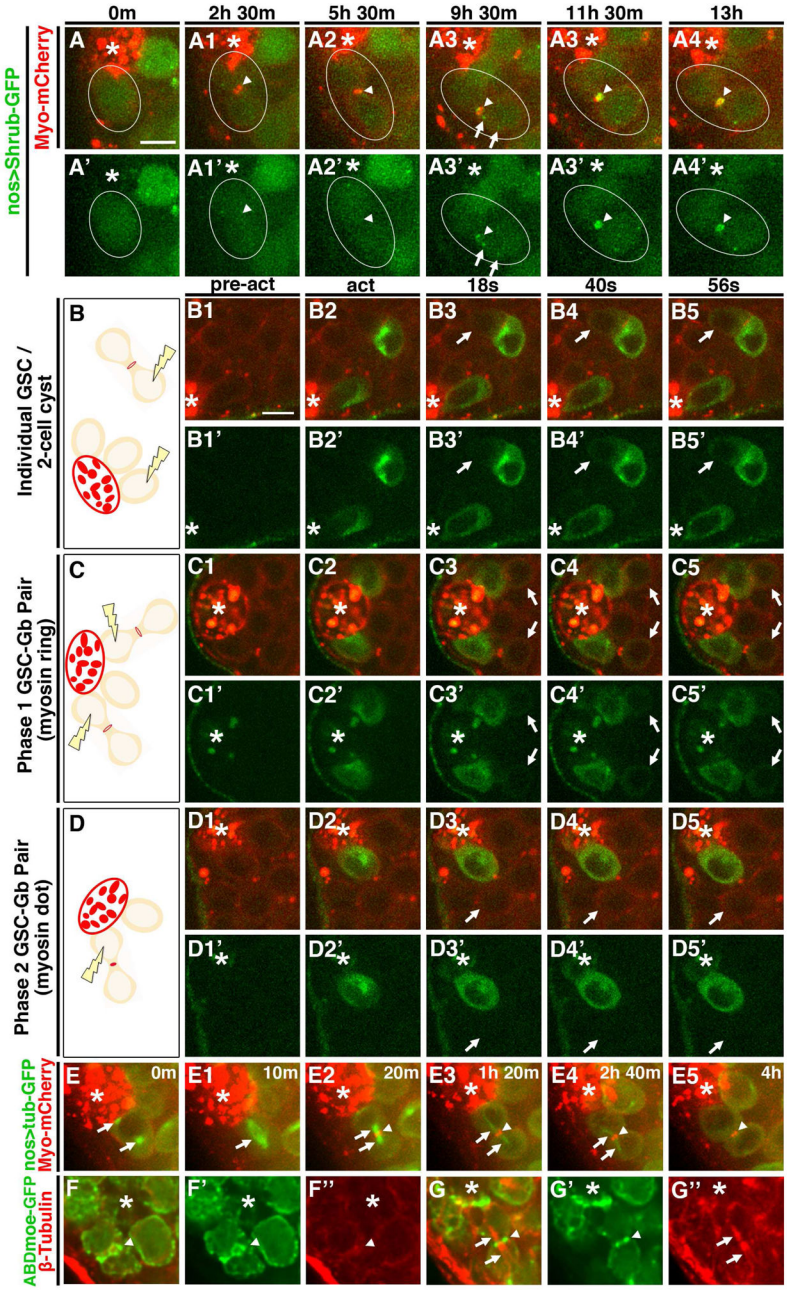


**Figure 2. Cytokinesis reinitiates during Phase Two**

(A1–A6′)Time lapse imaging of Shrub-GFP and Myo-mCherry. Each panel is a 3–5 Z plane projection. m=min. h=hour. Scale bar=5 microns. Arrowhead=IC bridge. Arrow=puncta of Shrub-GFP.

(B–D5′) Live imaging of germ cells expressing tubPA-GFP and Myo-mCherry before (pre-act), during (act) and after GFP photo-activation. Each panel is a single Z plane. Images taken every 2 seconds (s). Scale bar=5 microns. *=Hub. Arrow=attached, non-activated cell. (B, C, D) Diagrams showing positions of targeted cells.

(E1–E6) Live imaging of Tubulin-GFP and Myo-mCherry from mitosis through central spindle disassembly. Each panel is a 3–6 Z plane projection. *=Hub. m=min. Arrows=mitotic and central spindles. Arrowheads=IC bridge.
(M–N″) Immunofluorescent images of fixed testes stained for ABD-moeGFP and β-Tubulin (red). *=Hub. Each panel is a single Z plane. Arrowhead=IC bridge. Arrows=central spindle.

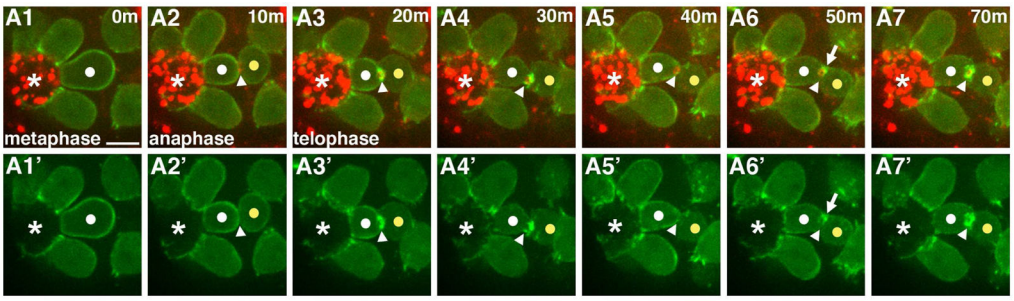


**Figure 3. Contractile ring disassembly and secondary ring formation in GSCs**

Time lapse imaging of GSC division; ABD-moeGFP and Myo-mCherry. Each panel is a 2–4 Z plane projection. (m=min). Images taken every 10 min. White dot=GSC. Yellow dot=Gb. Arrowhead=IC bridge. Arrow=F-actin foci. *=Hub. Scale bar=5 microns

See also Fig. S1.

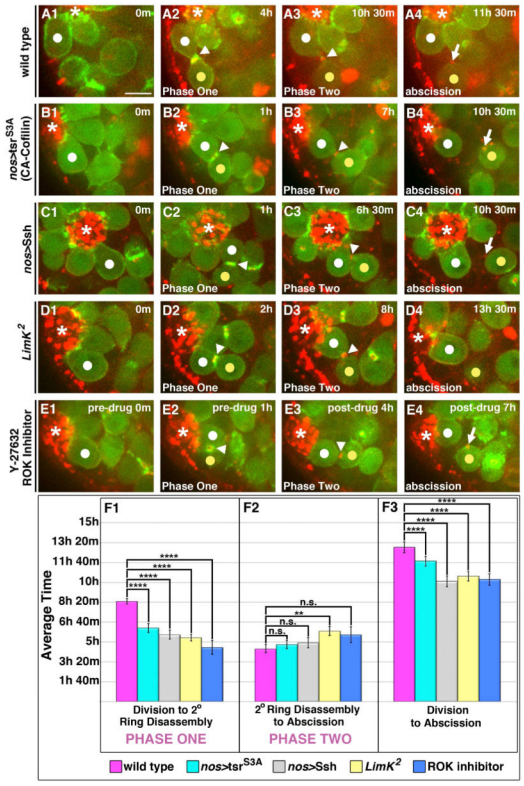


**Figure 4. Phase One is regulated by a ROK-LimK-Cofilin pathway**

(A1–E4)Time lapse imaging of GSC division cycle; ABD-moeGFP and Myo-mCherry. Each panel is a 3–5 Z plane projection. m=min. h=hour. White dot=GSC. Yellow dot=Gb. Arrowhead=IC bridge. Arrow=midbody remnant. *=Hub. Scale bar=5 microns

(A1–A4) GSC in wild type followed from division through abscission.

(B1–C4) GSCs expressing a constitutively active form of Cofilin (B1–B4) or the Cofilin phosphatase Ssh (C1–C4) followed from division through precocious abscission.

(D1–D4) GSC depleted of LimK followed from division through precocious abscission.

(E1–E4) GSC in testis treated with the Y-27632 ROK inhibitor followed form division through precocious abscission.

(F1–F3) Quantification of timing of indicated phases. (F1) Increased cofilin activity significantly shortened Phase One ($p<10^{-4}$ for all conditions). (F2) With the exception of *LimK*$^{2}$ mutants (p=0.001), the length of Phase Two remained unchanged in GSC-Gb pairs with increased Cofilin activity compared with wild type controls (*nos*>tsr$^{S3A}$ p=0.95; *nos*>Ssh p=0.31; ROK inhibitor p=0.05). (F3) The average time from division to abscission was significantly reduced in all GSC-Gb pairs with increased Cofilin activity compared with controls ($p<10^{-4}$ for all conditions). Data are represented as mean +/− SEM.

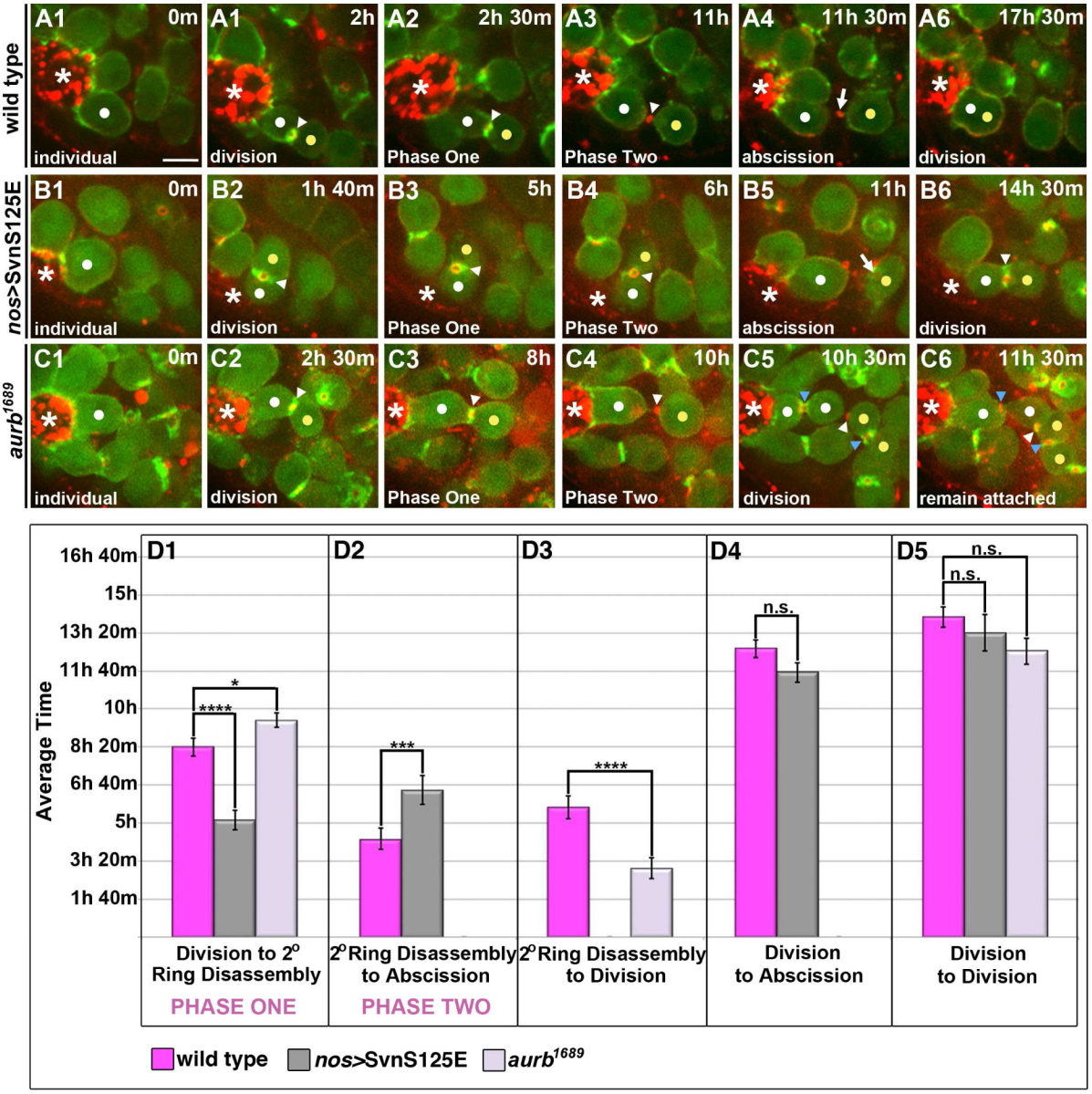


**Figure 5. AurB/Svn activity temporally regulates the transition between Phases One and Two of delay**

(A1–C6) Time lapse imaging of GSC division cycle; ABD-moeGFP and Myo-mCherry. Each panel is a 3–5 Z plane projection. m=min. h=hour. White dot=GSC. Yellow dot=Gb. White arrowhead="original" IC bridge. Blue arrowhead="new" IC bridge. Arrow=midbody remnant. *=Hub. Scale bar=5 microns

(A1–A6) Progression through two rounds of mitosis in a wild type GSC (same GSC images shown in Fig. 1).

(B1–B6) Progression through two rounds of mitosis in a GSC expressing SvnS125E that completes abscission.

(C1–C6) Progression through two rounds of mitosis in a GSC depleted of AurB that fails to complete abscission. The group of four cells (C5–C6) remained connected and associated

with the hub for the remainder of our imaging (1–3 hrs after second division). An F-actin ring was eventually reestablished at the “original” IC bridge (white arrowhead). (D1–D5) Quantification of timing of indicated phases. The same GSC-Gb pairs were followed through each stage reported. (D1) Expression of activated Svn led to precocious exit from Phase One ($p=3.6 \times 10^{-4}$) while depletion of Aurb had the reciprocal effect of prolonging Phase One (p=0.03). (D2) SvnS125E-expressing pairs spent a significantly longer time, on average, in Phase Two compared with controls ($p=9.0 \times 10^{-3}$). This likely reflects some conservation of the described role for AurB/Svn activity in delaying abscission. (D3) As GSCs depleted of AurB did not abscise, we instead quantified the time from secondary ring disassembly to division. Loss of AurB activity led to a statistically significant decrease in the average time from secondary ring disassembly to division compared with controls ($p=6.7 \times 10^{-4}$). (D4) The average time from division to abscission was not significantly different in SvnS125E-expressing pairs compared with controls (p=0.11) despite their precocious exit from Phase One. This is due to the increased length of Phase Two, which, as described above, reflects conservation of a role for the CPC in directly regulating abscission timing. (D5) GSCs followed through two rounds of mitosis revealed no significant difference in the cell cycle rate of GSCs expressing SvnS125E (p=0.43) or depleted of AurB (p=0.05) compared with controls. Data are represented as mean +/− SEM.

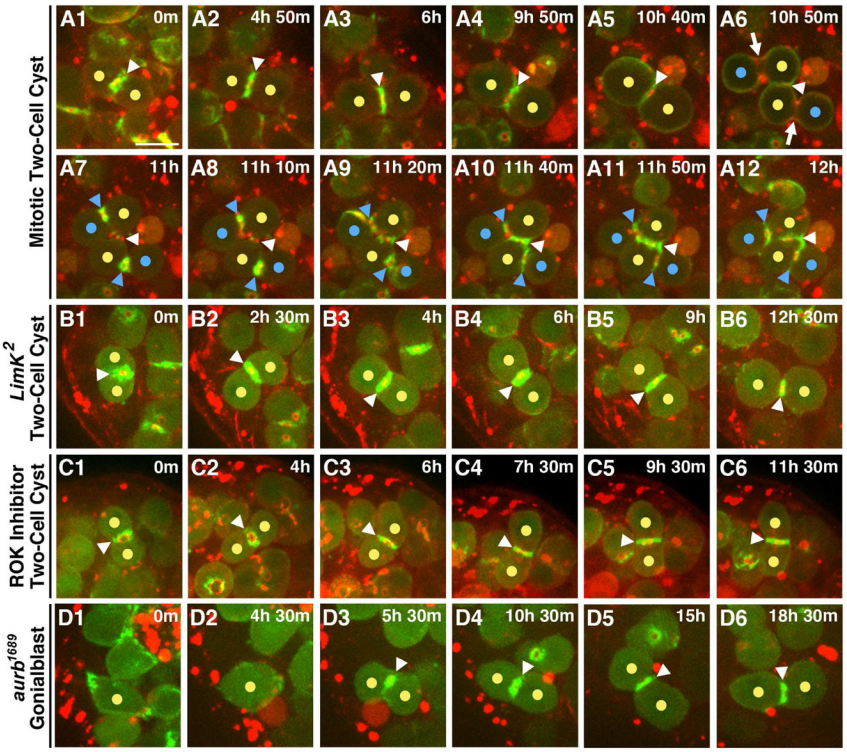


**Figure 6. Pathways regulating GSC cytokinesis are specific to the stem cell population**

Time lapse imaging of differentiating germ cell cysts; ABD-moeGFP and Myo-mCherry. Each panel is a 2–5 Z plane projection. Yellow dots=cells of two-cell cyst. White arrowhead="original" IC bridge. Blue dots=daughter cells formed during mitosis. Blue arrowheads="new" IC bridges. m=min. h=hour. *=Hub. Scale bar=5 microns.

(A1–A12)Division of a two-cell cyst. (A1–A4) The IC bridge of a two-cell cyst contained an F-actin ring for an extended period. (A5) F-actin at the IC bridge was only disassembled as the two cells rounded and entered mitosis. (A6) Myosin was enriched at the cleavage furrow during anaphase (arrows) between nascent daughter cells and a Myo-mCherry ring continued to mark the original IC bridge (arrowhead). (A7–A12) Contractile ring F-act is retained at the newly formed IC bridges of the four-cell cyst.

(B1–B6) Loss of LimK function has no effect on the F-actin ring at the IC bridge connecting two-cell cysts.

(C1–C6) Loss of ROK function has no effect on the F-actin ring at the IC bridge connecting two-cell cysts.

(D1–D6) As *aurb*$^{1689}$ is a hypomorphic allele, abscission is not disrupted in all GSC-Gb pairs and some individual Gbs are released. Loss of AurB activity does not disrupt formation or maintenance of the IC bridge connecting two-cell cysts.

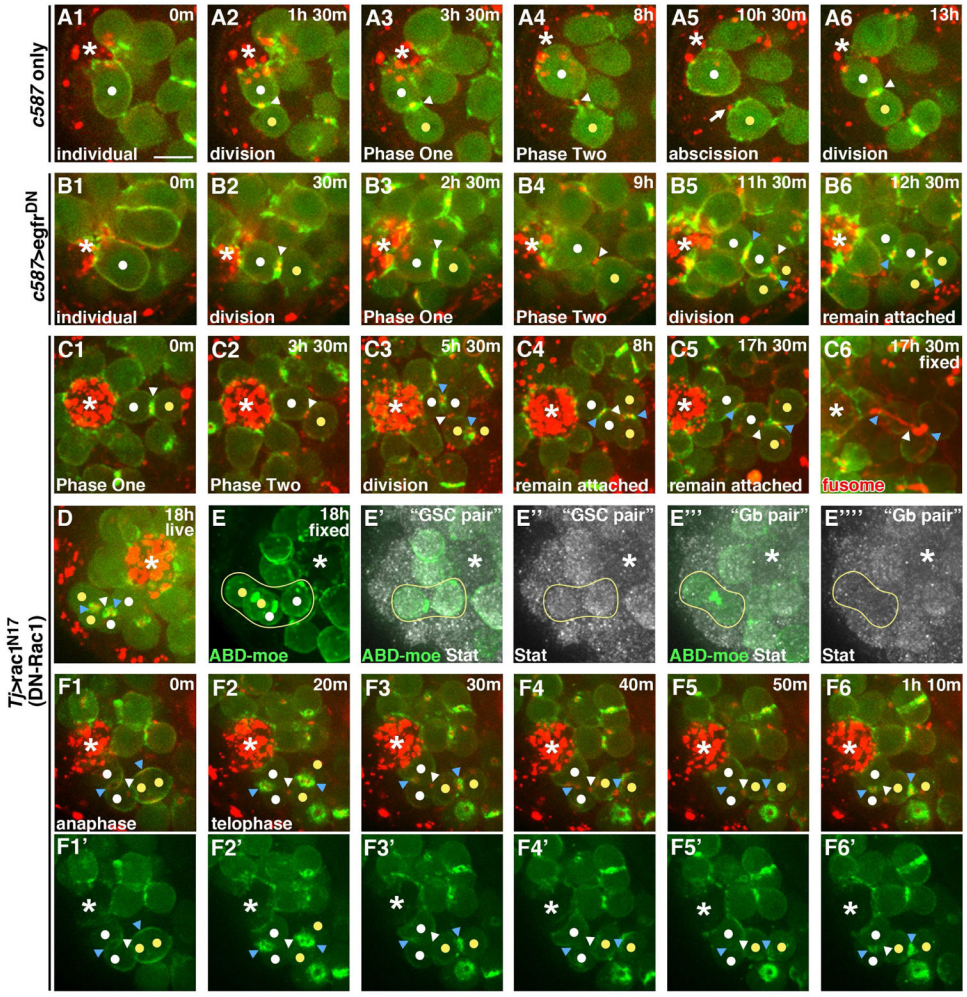


**Figure 7. Somatic cell encystment controls GSC-Gb abscission**

Time lapse imaging of ABD-moeGFP and Myo-mCherry in the indicated genotypes. Each panel is a 2–5 Z plane projection. m=min. h=hour. White dot=GSC and "new" GSC daughter generated after second division. Yellow dot=Gb and "new" Gb daughter generated after second division. White arrowhead="original" IC bridge. Blue arrowheads="new" IC bridges. Arrow=midbody remnant. *=Hub. Scale bar=5 microns.

(A1–A6) GSCs expressing the *c587* GAL4 driver only progressing through mitosis, abscission and a second mitosis.

(B1–B6) GSCs expressing a dominant-negative form of egfR using the *c587* driver. After a first cell division, the GSC-Gb pair fails to abscise so that following a second mitosis, an interconnected group of four cells is formed (B5) and retained (B6) at the hub.

(C1–C4) GSCs expressing a dominant-negative form of Rac1 using the *tj* driver. The GSC-Gb pair fails to abscise so that following a second mitosis, an interconnected group of four cells is formed (C3) and maintained (C4) at the hub.

(C5) Same GSC-Gb pair imaged (C1–C4) fixed and stained for GFP and the fusome (red).

(D) Last time point from live imaging of GSCs expressing dominant-negative Rac1 using the *tj* driver.

(E–E‴′) Imaged GSC (from D) fixed and stained. (E) Z projection showing all four interconnected cells attached to the hub. (E′–E″) Z projection of planes containing only the “GSC pair” (cell attached to hub and immediate daughter) showing Stat accumulation. (E‴–E‴′) Z projection of planes containing only the “Gb pair” (two cells most distal from hub in four-cell grouping) showing lack of Stat accumulation.

(F1–F6′) GSCs expressing a dominant-negative form of Rac1 using the *tj* driver with images collected every 10 min showing loss of contractile ring F-actin and formation of a secondary F-actin ring following division of attached GSC-Gb pair.